The Redox Chemistry of (N^1-[3-(2-aminoethylimino)-1,1-dimethylbutyl]ethane-1,2-diamine)nickel(II) Perchlorate, $Ni^{II}L^1(ClO_4)_2$, in Aqueous Solutions – A Pulse Radiolytic and an Electrochemical Study

Yael Albo,[a] Eric Maimon,*[a,b] Israel Zilbermann,[a,b] Magal Saphier,[a,b] Haim Cohen,[a,c] and Dan Meyerstein*[a,c]

Keywords: Nickel complexes / Pulse radiolysis / Electrochemistry

The ligand (N^1-[3-(2-aminoethylimino)-1,1-dimethylbutyl]-ethane-1,2-diamine), L^1, induces a high ligand field on the central Ni^{II} ion. Thus it is relatively easy to oxidize $(Ni^{II}L^1)^{2+}$. However, the kinetic stability of the $Ni^{III}L^1$ complexes is considerably lower than that of their analogous macrocyclic complexes. This difference in stabilities is attributed to the less rigid ligand framework, which facilitates the oxidation of ligand.

Introduction

The thermodynamic and kinetic stabilization of uncommon oxidation states of transition metal ions has been studied extensively. It has been suggested that for tetraaza aliphatic ligands a macrocyclic ligand frame sets the condition for the acceptance of high oxidation states,[1–3] which are not achievable in the case of the open tetraamine analogues. As a result there is not much information regarding the redox properties of transition metal complexes with open tetraamine ligands in aqueous solutions. Thus, there is an interest in expanding the knowledge of the ability of such ligands to stabilize uncommon oxidation states of transition metal ions. Herein the redox properties of the linear tetraamine Ni complex $Ni^{II}L^1(ClO_4)_2$ are investigated in aqueous solutions, and are compared to those of the tetraaza macrocyclic analogue $Ni^{II}L^2(ClO_4)_2$.

Results and Discussion

Characterization of $NiL^1(ClO_4)_2$

The complex was characterized by X-ray diffraction and by UV/Vis spectrophotometry. Spectral data of the complex at pH = 6.0 are summarized in Table 1. Spectral data of the $NiL^2(ClO_4)_2$ are included in the Table for comparison. It is interesting to note that the d-d bands of both complexes have the same λ_{max}, i.e. the two ligands impose the same ligand field on the central nickel ion. The electronic configuration of both complexes is low spin, i.e. the ligands impose a strong ligand field.

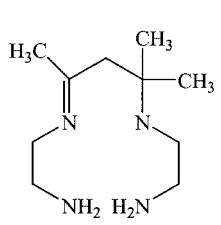

L^1

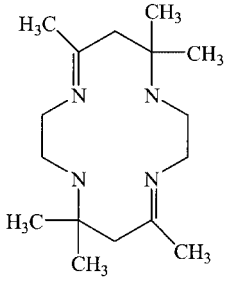

L^2

Table 1. UV/Vis spectrophotometric data for the $Ni^{II}L^1(ClO_4)_2$ and $Ni^{II}L^2(ClO_4)_2$ complexes.

	λ_{max} [nm]	ε [$M^{-1}cm^{-1}$]
$Ni^{II}L^1(ClO_4)_2$	436	70
	268	2000
	208	15000
$Ni^{II}L^2(ClO_4)_2$[18]	436	104
	238	7900
	213	17000

Crystal Structure

The ORTEP view of $[NiL^1(ClO_4)_2]$ is provided in Figure 1 and relevant geometric details are listed in Table 2. The complex is isolated as its perchlorate salt, and the Ni^{II} ion has a typical square-planar coordination geometry, as the bond angles N^1–Ni–N^4 and N^1–Ni–N^3 are 91.7° and 176°, respectively. The two perchlorate counterions are above and below the coordination plane, beyond bonding

[a] Chemistry Department, Ben Gurion University of the Negev, Beer Sheva, Israel
[b] Nuclear Research Centre Negev, Beer Sheva, Israel
E-mail: emymon@bgu.ac.il
[c] Biological Chemistry Department, College of Judea and Samaria, Ariel, Israel

distance. There is a hydrogen bonding interaction between the perchlorate counterions and the amines' hydrogen atoms of two neighboring complexes. These intermolecular interactions stabilize the structure of the complex. The Ni–N^3_{imine} bond length, 1.899 Å, is slightly shorter than the Ni–N^2_{amine} bond length. This is probably due to some back donation to the π system. The relative Ni–N bond lengths are clearly also affected by the N–H···O–Cl hydrogen bonds between the perchlorate anions and the N^1, N^2 and N^4 amines. The same effect was observed for the analogous macrocyclic complexes.[4]

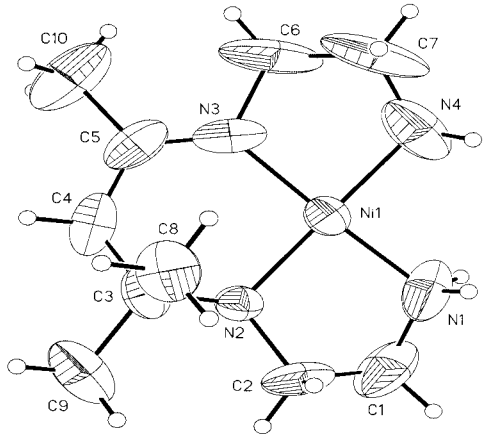

Figure 1. ORTEP view of $[NiL^1(ClO_4)_2]$, with displacement.

Table 2. Bond lengths [Å] and angles [°].

Ni(1)–N(1)	1.875(7)
Ni(1)–N(3)	1.899(8)
Ni(1)–N(2)	1.911(5)
Ni(1)–N(4)	1.910(7)
N(1)–Ni(1)–N(3)	176.6(4)
N(1)–Ni(1)–N(2)	87.6(3)
N(3)–Ni(1)–N(2)	95.0(3)
N(1)–Ni(1)–N(4)	91.7(4)
N(3)–Ni(1)–N(4)	85.7(4)
N(2)–Ni(1)–N(4)	179.3(4)

The small ellipsoids and the high order of the crystallographic structure indicate that only the R chiralic isomer was obtained, and not a racemic mixture of the two possible isomers.

Electrochemistry

A cyclic voltammetric study of $(NiL^1)^{2+}$ in aqueous solutions containing perchlorate and/ or sulfate ions was performed. The complex displays a quasi-reversible wave in the cyclic voltamogramm associated with the $Ni^{III/II}$ redox process. The redox potential of the couple in 0.1 M $NaClO_4$ is cathodically shifted by 250 mV relative to its tetraaza macrocyclic analogue,[5] $(NiL^2)^{2+}$, thus displaying a better ability of the open ligand frame to thermodynamically stabilize the trivalent state. This observation is probably due to contributions of the following factors:

a) The macrocyclic ligand contains two iminic bonds and is thus a softer base.

b) The macrocyclic complex has less hydrogen bonds with the solvent, i.e. is more hydrophobic.[6–9]

c) The open ligand is less rigid and thus has a better ability to satisfy the electronic and stereochemical demands of the central metal ion.

The redox potential in neutral solutions containing only $NaClO_4$ (0.1 M) is 950 mV vs. SCE. The complex is thermodynamically stabilized by sulfate ions (Figure 2), due to ligation of the anion to the complex $(NiL^1)^{3+}$. From the dependence of the redox potential on $[SO_4^{2-}]$ the slope of the plot of E vs. $\log[SO_4^{2-}]$ is 57 mV, thus it is concluded that the complex formed is $Ni^{III}L^1(SO_4)^+$ with an apparent stability constant $K_{app} = [(NiL^1SO_4)^+]/[(NiL^1)^{3+}][SO_4^{2-}] = 490 \pm 50\ M^{-1}$. This equilibrium constant was determined at pH = 6.0, as the divalent complex is unstable at lower pH values in sulfate containing solutions. The equilibrium constant for the macrocyclic complex $K = [\{NiL^2(SO_4)_2\}^-]/[(NiL^2)^{3+}][SO_4^{2-}]^2 > 10^5\ M^{-2}$ was obtained at pH = 1.2.[5] The lower value of the apparent equilibrium constant of the open complex probably stems from the higher pH value at which it was determined, as the equilibrium constant is pH dependent, as shown by the following relations:

$$NiL^1(H_2O)^{3+} \rightleftharpoons NiL^1OH^{2+}_{(aq)} + H^+_{(aq)}$$

$$K_1 = \frac{[(NiL^1OH)^{2+}][H^+]}{[(NiL^1)^{3+}]}$$

$$(NiL^1)^{3+}_{(aq)} + SO_4^{2-}{}_{(aq)} \rightleftharpoons NiLSO_4^+{}_{(aq)}$$

$$K_2 = \frac{[(NiL^1SO_4)^+]}{[(NiL^1)^{3+}][SO_4^{2-}]}$$

Combining the two equations:

$$K_2 = \frac{[(NiL^1SO_4)^+]K_1}{[SO_4^{2-}][(NiL^1OH)^{2+}][H^+]}$$

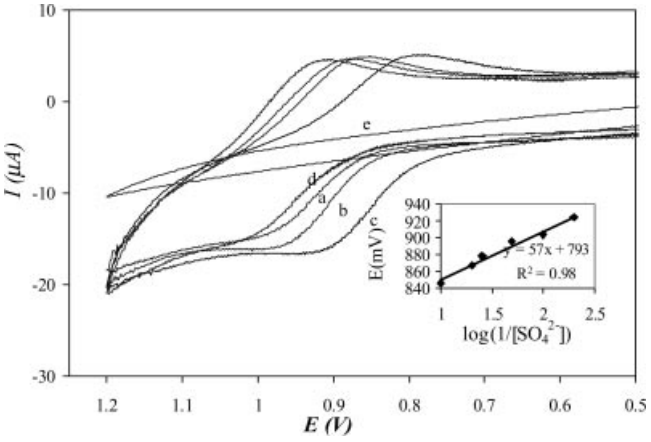

Figure 2. Cyclic voltammograms of the couple $Ni^{III/II}L^1$ in sulfate-containing solutions. Conditions: working electrode glassy carbon, reference SCE, scan rate 150 mV/s, ionic strength regulated with $NaClO_4$: $1 \cdot 10^{-3}$ M $Ni^{II}L^1$(a–d), 0.005 M Na_2SO_4 (a), 0.01 M Na_2SO_4 (b), 0.04 M Na_2SO_4 (c), 0.15 M $NaClO_4$ (d), 0.1 M Na_2SO_4 (e), pH = 6, I = 0.15.

The observation that two sulfate ions ligate to the macrocyclic complex, in comparison to the open complex, to

which only one sulfate ion ligates might be attributed to the fact that the less rigid open ligand enables a tetragonal bipyramid conformation which is not possible for the macrocyclic complex.

Pulse Radiolysis Studies

The redox properties of the complex were further investigated using the pulse radiolysis technique. N_2O-saturated solutions in the presence and absence of bromide ions were irradiated.

Oxidation of the Complex by Hydroxyl Radicals

When N_2O-saturated solutions containing $(2–25)\cdot10^{-5}$ M $Ni^{II}L^1(ClO_4)_2$ are irradiated three consecutive reactions are observed. The rate of the formation of the first trivalent transient obeys a pseudo-first order rate law, Figure 3. From the linear dependence of the observed rate on $[(Ni^{II}L^1)^{2+}]$, a rate constant of $(5.0\pm1.0)\cdot10^9$ $M^{-1}s^{-1}$ is determined. The trivalent complex is obtained via:[10]

$$H_2O \xrightarrow{e,\gamma} e^-_{aq}(2.65), H^{\cdot}(0.60), {}^{\cdot}OH(2.65), H_2(0.45), H_2O_2(0.75)$$

where the values in parentheses give the relative yields of the primary products, number of molecules formed per 100 eV absorbed in the solution.

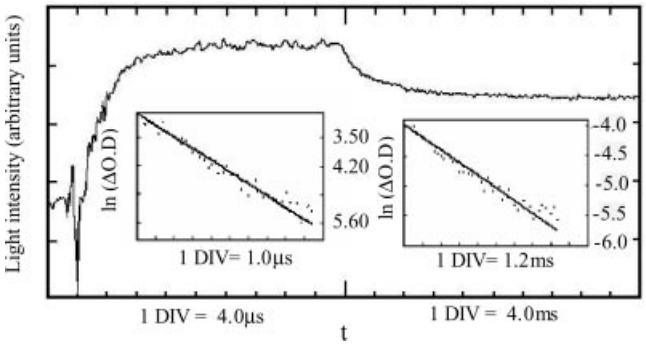

Figure 3. The formation and isomerization kinetics of $Ni^{III}L^1$. Conditions: $5.0\cdot10^{-5}$ M $(Ni^{II}L^1)^{2+}$, pH = 3.8, λ = 525 nm, N_2O-satd., pulse intensity 8.1 Gy.

$$e^-_{aq} + N_2O + H_2O \rightarrow N_2 + {}^{\cdot}OH + OH^- \quad (1)$$
$$k_1 = 8.7\cdot10^9\ M^{-1}s^{-1}[11]$$

$$Ni^{II}L^1 + {}^{\cdot}OH \rightarrow Ni^{III}L^1{}_{aq} + OH^- \quad (2)$$
$$k_2 = 5.0\cdot10^9\ M^{-1}s^{-1}$$

(The rate of the analogous reaction for the macrocyclic complex is $9\cdot10^9$ $M^{-1}s^{-1}$.[12]) The second reaction, which obeys a first order rate law with a rate which is independent of the complex concentration, causes a significant change in the spectrum of the $Ni^{III}L^1{}_{aq}$ complex (Figure 4). This reaction is attributed to the isomerization of the complex from a pentacoordinated geometry to an octahedral geometry in analogy[12] to the observations for $Ni^{III}L^2{}_{(aq)}$.

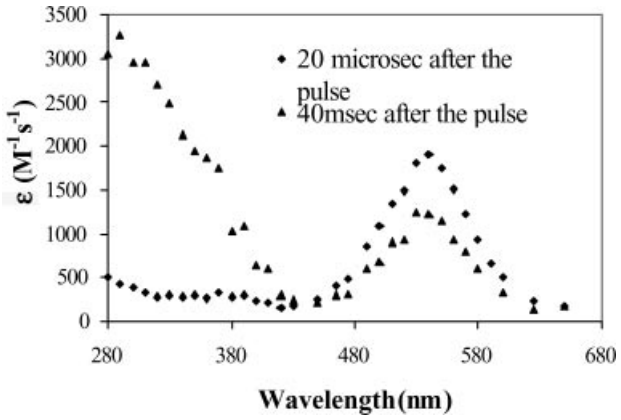

Figure 4. Spectra of $Ni^{III}L^1$ and $(Ni^{III}L^1)_R$. Conditions: $1\cdot10^{-4}$ M $(Ni^{II}L^1)^{2+}$, pH = 4.0 N_2O-satd., pulse intensity: 7.2 Gy.

The absorbance of the product of reaction (3), $(Ni^{III}L^1)_R$, depends on the pH value (Figure 5). The results indicate a pK_a of 4.3 ± 0.2 for the complex formed after the first reaction, reaction (2). It is suggested that this pK_a is due to equilibrium (4). The pK_a value for the complex with the macrocyclic ligand is lower (3.4).[12] The strong absorption band of $Ni^{III}L^1(OH)^{2+}$ at 540 nm is attributed to a d-d transition in the highly unsymmetrical $Ni^{III}L^1(OH)^{2+}$ complex. It is thus found that the basic complex $Ni^{III}L^1(OH)^{2+}$ does not isomerize. Again this finding is analogous to that reported earlier for $Ni^{III}L^2(OH)^{2+}$.[12]

$$Ni^{III}L^1\ aq \rightarrow (Ni^{III}L^1aq)_R \quad (3)$$
$$k_3 = 190\ s^{-1}$$

$$(Ni^{III}L^1)_{aq}{}^{3+} \rightleftharpoons Ni^{III}L(OH)^{2+} + H_3O^+ \quad (4)$$

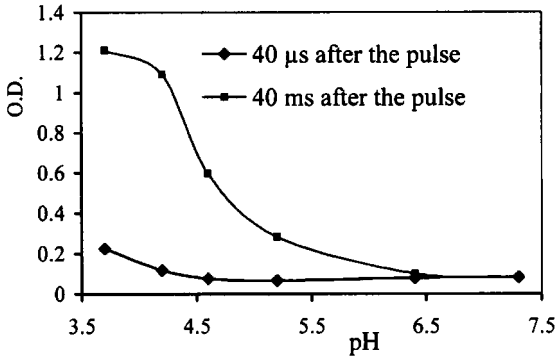

Figure 5. Optical densities of transient as a function of the pH value. Conditions: $2.5\cdot10^{-4}$ M $(Ni^{II}L^1)^{2+}$, λ = 300 nm, N_2O-satd., pulse intensity 32 Gy.

Clearly the formation of the red Ni^{III} transient in this study is not due to the macrocyclic effect and not to the favorable preorientation of the donor atoms in the 14-membered tetraaza macrocyclic ligand as proposed in the literature.[13]

The third reaction occurs on a time scale of seconds, obeys a second order rate law and is base catalyzed. This reaction results in the disappearance of the spectrum of the in-

termediate and is attributed to the decomposition of the trivalent complex. It is proposed that the decomposition mechanism is as described in reaction (5).

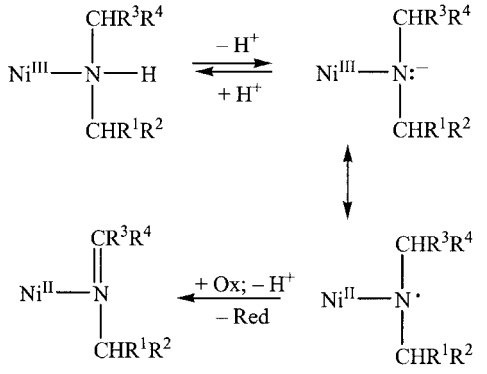

(5)

A linear dependence of the observed second-order rate constant on [OH^-] is observed, but the slope is 0.25 (Figure 6), i.e. considerably smaller than a slope of 1 which is expected according to this mechanism. This discrepancy is attributed to the pK_a of the tervalent complex, reaction (4) and probably to another pK_a i.e. to the formation of $Ni^{III}L^1(OH)_2^+$. Alternatively there is another decomposition mechanism, which does not require the loss of a proton.

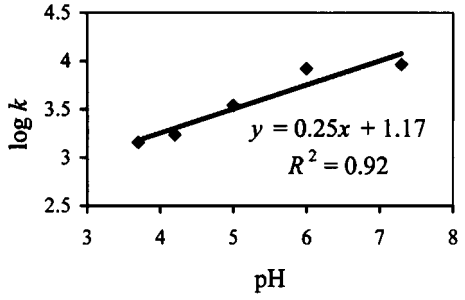

Figure 6. Decomposition rate constant as a function of the pH value. Conditions: $2.5\cdot10^{-4}$ M $(Ni^{II}L^1)^{2+}$, N_2O-satd., pulse intensity: 7.2 Gy.

The oxidation mechanism by the hydroxyl radicals and the mechanism of decomposition of the trivalent complex and its products are similar to those of its macrocyclic analogue.[12] However the oxidation product of $(Ni^{II}L^1)^{2+}$ is less stable.

Oxidation of the Complex by $Br_2^{\cdot-}$ Ion Radicals

As hydroxyl radicals might, at least partially, react also via hydrogen abstraction from the organic ligands it was decided to use also $Br_2^{\cdot-}$ as an oxidizing agent [$E^0(Br_2^{\cdot-}/2Br^-)$ = +1.63 V vs. N.H.E[11]]. N_2O-saturated solutions containing 0.01–0.1 M NaBr, $(0.1–2.0)\cdot10^{-4}$ M $Ni^{II}L^1(ClO_4)_2$ were irradiated. The first reaction observed obeys a first order rate law, with a rate proportional to $[(Ni^{II}L^1)^{2+}]$. The spectrum of the transient formed in this reaction differs considerably from that of $(Ni^{III}L^1)^{3+}$, Figure 7 and 4, and therefore it is proposed that $Ni^{III}LBr^{2+}$ is formed in this reaction, see (8).

$$^{\cdot}OH + Br^- \rightleftharpoons OHBr^{\cdot-} \quad (6)$$

$$OHBr^{\cdot-} + Br^- + H^+ \rightarrow Br_2^{\cdot-} + H_2O \quad (7)$$

$k > 10^9$ M^{-1}s^{-1} at pH $\leq$ 9.5

$$(Ni^{II}L^1)^{2+} + Br_2^{\cdot-} \rightarrow (Ni^{III}L\text{–}Br)_{aq}^{2+} + Br^- \quad (8)$$

$k = (7.5\pm2.0)\cdot10^9$ M^{-1}s^{-1}

(The rate of the analogous reaction for the macrocyclic complex is $2.5\cdot10^9$ M^{-1}s^{-1}.[12])

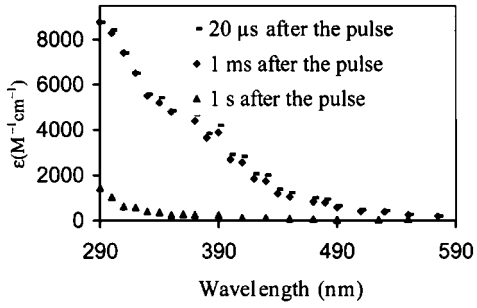

Figure 7. Spectra at different times after the pulse in the bromide-containing system. Conditions: $1\cdot10^{-4}$ M $(Ni^{II}L^1)^{2+}$, 0.1 M NaBr (for the micro- and milliseconds time scales), 0.01 M NaBr (1 second after the pulse), pH = 3.8, N_2O-satd., pulse intensity 8.2 Gy.

The second reaction observed also obeys a first order rate law and its rate is proportional to [Br^-], Figure 8; the large intercept suggests that this is an equilibrium process, see (9).

$$(Ni^{III}L^1Br)^{2+}_{(aq)} + Br^- \rightleftharpoons Ni^{III}L^1Br_2^+ \quad (9)$$

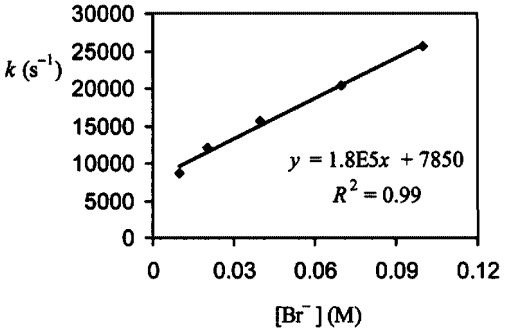

Figure 8. Observed rate as a function of [Br^-]. Conditions: $1\cdot10^{-4}$ M $(Ni^{II}L^1)^{2+}$, (0.01–0.1) M NaBr, pH = 3.8, ionic strength of 0.1 M adjusted by $NaClO_4$, N_2O-satd., pulse intensity 7.1 Gy, λ = 500 nm.

The spectrum of the product of the transient formed in reaction (9) is very similar to that formed in reaction (8), Figure 7. This is reasonable as the major band observed is clearly due to a LMCT transition. The slight shift to the blue is attributed to the lowering of the redox potential of the $Ni^{III/II}$ couple by the binding of a second bromide. From the slope and intercept in Figure 8 one obtains $k_9 = (1.8\pm0.2)\cdot10^5$ M^{-1}s^{-1} and $K_9 = 23\pm10$ M^{-1}.

The oxidation mechanism by the $Br_2^{\cdot-}$ ion radicals of the macrocyclic complex is different. In this case only one bromide ion ligates as an axial ligand, and the number of reac-

tions occurring and the reaction rate constants are pH-dependent.[12]

The decomposition reaction of $Ni^{III}L^1Br_2^+$ obeys a second order rate law, with a rate independent on the divalent complex concentration and weakly dependent on pH and bromide concentration [k = $9.9\cdot10^5$ $M^{-1}s^{-1}$, $2\cdot10^{-4}$ M $(Ni^{II}L^1)^{2+}$, 0.01 M NaBr, pH = 3.8; k = $9.8\cdot10^5$ $M^{-1}s^{-1}$, $1\cdot10^{-4}$ M $(Ni^{II}L^1)^{2+}$, 0.01 M NaBr, pH = 3.8; k = $3.6\cdot10^6$ $M^{-1}s^{-1}$, $1\cdot10^{-4}$ M $(Ni^{II}L^1)^{2+}$, 0.1 M NaBr, pH = 3.8; k = $1.7\cdot10^4$ $M^{-1}s^{-1}$, $1\cdot10^{-4}$ M $(Ni^{II}L^1)^{2+}$, 0.01 M NaBr, pH = 7.0]:

$$2\ Ni^{III}L^1Br_2^{+} \longrightarrow \begin{cases} 2\ (Ni^{II}L^1)^{2+} + Br_2 + 2\ Br^- \ (Br^- + BrO^-) \\ (Ni^{II}L^1)^{2+} + Ni^{II}L_{-2H}^{2+} + 4\ Br^- + H^+ \end{cases} \quad (10)$$

The mechanism of decomposition of the trivalent macrocyclic complexes in the presence of bromide differs considerably. Comparison of the decomposition reaction shows that the rate of decomposition in the case of the open ligand is slightly higher at acidic pH values, and is much higher in neutral solutions than that of the analogous macrocyclic complex. The dependence of the rate on the bromide concentration is smaller in the case of the open ligand frame, both in acidic and neutral solutions. For the open ligand the decomposition reaction is second order in the whole pH range, while it is first order in neutral solution in the macrocyclic system. The difference in the kinetic stabilities of the two complexes is attributed to the less rigid frame of the open ligand. The formation of $Ni^{II}L_{-2H}^{2+}$ requires the formation of a C–N double bond, i.e. a significant change in geometry, which is facilitated by the less rigid open ligand.[14] This conclusion is in agreement with the observation that the stabilities of the isomers of Ni^{III}(5,7,7,12,14,14-hexamethyl-1,4,8,11-tetraaazacyclotetradecane) differ considerably.[15]

Concluding Remarks

In conclusion it was found that the less rigid open ligand has a better ability to adjust itself to the structure of each valence, and as such it thermodynamically stabilizes the trivalent state better than its macrocyclic analogue, although the oxidation product is less kinetically stable.

Experimental Section

Materials: All the chemicals used were of AR grade and were used without further treatment. All solutions were prepared with deionized water, which was further purified by passing through a Millipore Milli-Q water purification system, the final resistance being above 10 MΩ

Synthesis of $NiL^1(ClO_4)_2$: 0.2 mol $Ni(ClO_4)_2\cdot6H_2O$ and 0.4 mol of ethylenediamine were added to an excess of acetone (as the solvent). The solution was stirred and heated under reflux for 4 days. The first crude orange crystals formed were filtered and washed in methanol. Single crystals suitable for X-ray diffraction were obtained from recrystalization in methanol.

The tetrachlorozincate salt of this complex was synthesized by Curtis and House using a different procedure.[16]

Electrochemical Measurements: Electrochemical studies were carried out using an EG&G Princeton Applied Research potentiostat/galvanostat, Model 263, operated by a Research Electrochemistry software EG&G PARC, using a three electrode assembly consisting of a glassy carbon electrode (A = 0.07 cm^2), a Pt wire auxiliary electrode and a SCE as the reference electrode. The solutions were purged with argon.

Pulse Radiolysis: The solutions were handled by the syringe technique. Deaeration was performed by bubbling N_2O through the solutions.

The experiments were carried out at the linear electron accelerator facility of the Hebrew University of Jerusalem; 0.5–1.5 μs, 5 MeV and 200 mA pulses were used. The dose per pulse was in the range of 7–32 Gy/pulse. The experimental setup and the techniques used for evaluating the results have been described elsewhere in detail.[17]

X-ray Structure Determination: The data were collected on a Bruker SMART system with 1 K CCD detector. Mo-$K\alpha$ radiation was used with a graphite monochromator. The data were reduced using SAINT, absorption corrections were performed using SADABS, and then solved with SHELXL and refined using SHELXL. The non-hydrogen atoms were located from the difference map and refined anisotropically. The hydrogen atoms were located from the difference map and then allowed to refine using a riding model. An ORTEP view of the molecules is provided in Figure 1, and geometry details are listed in Table 2.

***C*rystal and Structure Refinement Data:** Crystal data $[NiL^1(ClO_4)_2]$: $C_{10}H_{24}Cl_2N_4NiO_8$ (457.92), monoclinic, space group $P21/c$, a = 10.3442(17), b = 12.540(2), c = 14.381(2) Å, $\alpha = \gamma$ = 90°, β = 101.795(5)°, V = 1826.1(5) $Å^3$, D_c (Z = 4) = 1.658 g/cm^3, crystal size $0.97\times0.77\times0.41$ mm^3, hkl range –8 to 13, –16 to 16, –19 to 19, N = 14613, N_{ind} = 4538 (R_{int} = 0.0412), residuals $R_1(F)$ 0.0674, wR_2 = 0.2067, GoF(all) = 1.307, Dr (min./max.) = 0.964/–0.664 $e\cdot A^3$.

CCDC-238587 contains the supplementary crystallographic data for this paper. These data can be obtained free of charge from the Cambridge Crystallographic Data Center via www.cccdc.cam.ac.uk/data_request/cif.

Acknowledgments

We thank Dr. Janice Rubin-Preminger for her X-ray structure determination. This study was supported in part by a grant from the Budgeting and Planning Committee of the Council of Higher Education and the Israel Atomic Energy Commission. D. M. wishes to express his thanks to Mrs. Irene Evens for her ongoing interest and support.

[1] I. Zilbermann, G. Golub, H. Cohen, D. Meyerstein, *J. Chem. Soc., Dalton Trans.* **1997**, *2*, 141–143.
[2] F. V. Lovecchio, E. S. Gore, D. H. Busch, *J. Am. Chem. Soc.* **1974**, *96*, 3109–3118.
[3] A. Bencini, L. Fabbrizzi, A. Poggi, *Inorg. Chem.* **1981**, *20*, 2544–2549.
[4] D. J. Szalda, E. Fujita, *Acta Crystalografica, Sect. C: Crystal Structure Communications* **1992**, *48*, 1767–1771.
[5] E. Zeigerson, G. Ginzburg, *J. Electroanal. Chem.* **1981**, *127*, 113–126.

[6] I. Zilbermann, E. Maimon, H. Cohen, D. Meyerstein, *Chem. Rev.* **2005**, *105*, *2609*–2625.
[7] D. Meyerstein, *Coord. Chem. Rev.* **1999**, *186*, 141–147.
[8] G. Golub, H. Cohen, P. Paoletti, A. Bencini, A. Messory, I. Bertini, D. Meyerstein, *J. Am. Chem. Soc.* **1995**, *117*, 8353–8361.
[9] T. Clark, M. Hennemann, R. van Eldik, D. Meyerstein, *Inorg. Chem.* **2002**, *41*, 2927–2935.
[10] L. J. Kirschenbaum, D. Meyerstein, *Inorg. Chem.* **1980**, *19*, 1973.
[11] G. V. Buxton, C. L. Greenstock, W. P. H. Helman, A. R. Ross, *J. Phys. Chem. Ref. Data* **1988**, *17*, 513.
[12] M. Jaacobi, D. Meyerstein, J. Lillie, *Inorg. Chem.* **1979**, *18*, 429–433.
[13] G. De Santis, L. Fabbrizzi, A. Poggi, A. Taglietti, *Inorg. Chem.* **1994**, *33*, 134–139.
[14] D. Shamir, I. Zilbermann, E. Maimon, D. Meyerstein, *Eur. J. Inorg. Chem.* **2004**, 4002–4005.
[15] E. Zeigerson, G. Ginzburg, J. Y. Becker, L. J. Kirschenbaum, H. Cohen, D. Meyerstein, *Inorg. Chem.* **1981**, *20*, 3988–3992.
[16] D. A. House, N. F. Curtis, *J. Am. Chem. Soc.* **1962**, *84*, 3248–3250.
[17] S. Goldstein, G. Czapski, H. Cohen, D. Meyerstein, *Inorg. Chem.* **1992**, *31*, 2439–2444.
[18] E. Zeigerson, Ph. D. Thesis, Ben-Gurion Gurion University of the Negev, Beer-Sheva, **1980**

Received: June 6, 2005
Published Online: September 13, 2005

